RESEARCH PAPER

Human Vaccines & Immunotherapeutics 9:4, 773–783; April 2013; © 2013 Landes Bioscience

Synergistic effect of methionine encephalin (MENK) combined with pidotimod(PTD) on the maturation of murine dendritic cells (DCs)

Yiming Meng,[1] Qiushi Wang,[3] Zhenjie Zhang,[1] Enhua Wang,[2] Nicollas P. Plotnikoff[4] and Fengping Shan[1,*]

[1]Department of immunology; School of Basic Medical Science; China Medical University; Shenyang, P.R. China; [2]Institute of pathology and pathophysiology; School of Basic Medical Science; China Medical University; Shenyang, P.R. China; [3]Central Blood Bank; Shengjing Hospital; China Medical University; Shenyang, P.R. China; [4]TNI Biotech. Company; Bethesda, MD USA

Keywords: MENK, PTD, synergistic effect, BMDCs, maturation

Abbreviations: MENK, methionine enkephalin; PTD, pidotimod; ACP, acidic phosphatase; DCs, dendritic cells; BMDCs, bone-marrow derived dendritic cells; LPS, lipopolysaccharide; SEM, scanning electron microscopy; TEM, transmission electron microscopy; DAB, 3, 3'-diaminobenzidine; MTS, 3-(4,5-dimethylthiazol-2-yl)-5-(3-carboxy-methoxyphenyl)-2-(4-sulfophenyl)-2H-tetrazolium, inner salt; PMS, phenazinemethosulphate; MACS, magnetic activated cell sorting; FACS, fluorescence activated cell sorting; GM-CSF, granulocyte macrophage–colony-stimulating factor; HRP, horseradish peroxidase; PBS, phosphate balanced solution

To gain new insight into the functional interaction between dendritic cells and methionine encephalin (MENK) combined with pidotimod (PTD), we have analyzed the effect of MENK plus PTD on the morphology, phenotype and functions of murine bone-marrow derived dendritic cells (BMDCs) in vitro. The maturation of BMDCs cultured in the presence of either MENK or PTD alone, or MENK in combination with PTD, was detected. The cell proliferation was measured by 3-(4,5-dimethylthiazol-2-yl)-5-(3-carboxy-methoxyphenyl)-2-(4-sulfophenyl)-2H-tetrazolium, inner salt/phenazinemethosulphate (MTS/PMS). The changes of BMDCs morphology were confirmed with light microscopy, transmission electron microscopy (TEM) and scanning electron microscopy (SEM). The BMDCs treated with MENK combined with PTD displayed a higher expression of typical maturation markers of CD40, CD80, CD83, CD86 and MHC-II identified by fluorescence activated cell sorting (FACS), and stronger ability to drive T cells. The decrease of the endocytic ability was assayed by DAB kit, FITC-dextran and cellular immunohistochemistry. Finally upregulation of cytokines production of IL-12 and TNF-α was determined by ELISA. These data indicate that MENK combined with PTD could exert synergistic action on BMDC maturation.

Introduction

Endogenous opioid peptides, discovered by Hughes and coworkers[1] in 1975, are known to be potent regulators of growth[2-4] as well as neuromodulators/neurotransmitters.[5,6] Initially studied for the role of native opioid peptides as neurotransmitters, endogenous opioids have been shown to be present in neural and non-neural tissues, and evoked a number of functions other than neuromodulation.[7,8] One well-studied role of enkephalins, especially methionine encephalin (MENK), encoded by the preproenkephalin A (PPE) gene, termed opioid growth factor (OGF) was that of growth regulation.[9] This peptide, MENK arises via autocrine and possibly paracrine pathways and is produced, secreted, and effective at concentrations consistent with its growth effects and binding affinity of its receptor-OGF receptor. MENK, via binding to multiple opioid receptors (μ,δ,κ) regulates a wide variety of physiological functions and is a tonic inhibitory peptide in cell proliferation and tissue organization during development, cancer, cellular renewal, wound healing, and angiogenesis.[10-14]

Pidotimod [PTD, (R)-3-[(S)-(5-oxo-2-pyrrolidinyl) carbonyl]-thiazolidine-4-carboxylic acid] is the first compound of a new class of biological response modifiers with a peptide-like structure with biological and immunological activity on both the adaptive and the innate immune responses.[15,16] In vitro studies, both from animals and human specimens, have documented good activity on innate and adaptive immune responses, and have been confirmed by in vivo studies. The previous studies also demonstrated that PTD itself did not have antibacterial activity, but when combined with antibacterial agents could be effective in improving clinical symptoms of patients, promoting recovery and shortening hospital stay. In particular, administration of PTD by the oral route could increases resistance to viral infections and make the activity of antiviral drugs more active for recurrent respiratory infections (RRI).[17-19] However,

*Correspondence to: Fengping Shan; Email: shantnib@163.com.
Submitted: 08/27/12; Revised: 11/26/12; Accepted: 12/06/12
http://dx.doi.org/10.4161/hv.23137

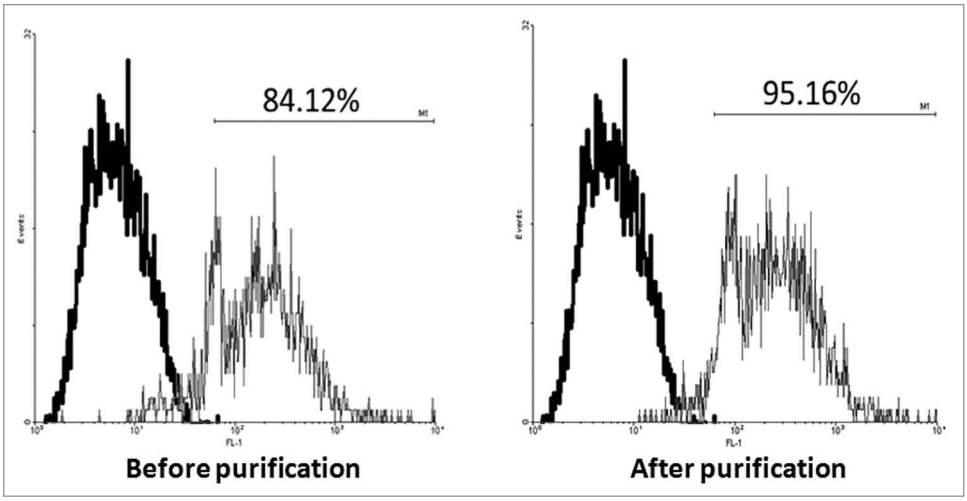

Figure 1. MACS. Bone marrow cells were obtained from femurs and tibias of 4- to 6-week-old female C57BL/6 mice post incubation with 10 ng/ml recombinant murine GM-CSF and 10 ng/ml IL-4. At the end of culture period, all cells expressing CD11c in the different wells were isolated respectively using MACS. Purified cells were routinely > 95% CD11c. Bold line histograms show the background staining with isotype control mAbs, and thin line histograms represent CD11c staining.

the effects of PTD on cellular immune response are still poorly characterized.

Dendritic cells (DCs) are immunological sentinels of the organism acting as antigen-presenting cells (APC), which can process antigen and present them to T cells, playing a key role in the initiation and regulation of immune responses.[20] DCs reside in a resting or immature state in peripheral tissues where they can efficiently capture and process Ag. Upon activation they initiate a differentiation process that results in decreased Ag-processing capacities, enhanced expression of MHC and co-stimulatory molecules, and migration into secondary lymphoid organs, where they trigger naïve T cells and induce Th1 or Th2 polarization depending on the pathological context. Ag-processing and T-cell sensitization are both essential for the development of antitumor immunity. So it is crucial to understand the regulation of DC maturation to gain further insight into their in vivo function.[21-25] Both MENK and PTD are peptide molecules of TH1 modulatiors,[5,16] and each of these peptides, when used separately, promotes functional maturation of dendritic cells and have a marked effect on suppressing the progression of some tumors.[26,27] Whether these two peptides exert synergistic effect on DCs remains unclear so far. The purpose of this study was to investigate the effect of MENK, when combined with PTD on maturation of DC, to provide a key reference for combined use of them in clinical treatment or preparation of vaccines.

Results

MACS. At the end of culture period, the BMDCs were positively purified using anti-CD11c MicroBeads, and a magnetic cell sorting column. The purity of BMDCs was > 95% as determined by CD11c staining (**Fig. 1**) (the gating strategy used for data analysis was to restrict the analysis to live singlets of CD11c-positive cells).

Proliferation assay. The results of BMDCs treated with graded concentrations of MENK or PTD were shown in **Figure 2A and B**. Significant increases in the number of viable cells were observed at 48 h after addition of 10^{-12}M MENK or 1.1 μg/ml PTD. Furthermore, with use of optimal concentrations of 10^{-12}M of MENK and 1.1 μg/ml of PTD at different time point, the optimal stimulating time at which the MENK or PTD could markedly promote proliferation with statistical significance ($^*p < 0.05$) was obtained (**Fig. 2C and D**). After that, the purified BMDCs treated with LPS, 10^{-12}M MENK (M), 1.1 μg/ml PTD (P), and the 10^{-12}M MENK plus 1.1 μg/ml PTD for 48h (**Fig. 3**) were also measured by MTS assay. These results showed that MENK plus PTD could markedly increase the absolute number of BMDCs in a synergistic way as compared with that stimulated with MENK or PTD alone ($^*p < 0.05$, $^{**}p < 0.01$).

Morphology under light microscopy. The progenitor cells from the bone marrow cells of C57BL/6 mice were cultured in the presence of GM-CSF and IL-4 for 7 d to induce their development, and then the cells were treated with different drugs respectively for 48 h before the BMDCs were observed under light microscopy. The results demonstrated that the BMDCs in the RPMI 1640 group were small and round with smooth boundaries or prolongations. In contrast the cells in the testing group, showed large cells with oval or irregularly shaped nuclei and the increased short and blunt dendritic processes radiated from many cell surface (**Fig. 4**).

Morphology under TEM. BMDCs incubated with GM-CSF and IL-4 for 7 d and then in the absence or presence of the testing drugs for 48 h were observed under TEM. The immature BMDCs, in the RPMI 1640 group, exhibited areas of vesicles and, a less irregular surface with less cytoplasmic and small eletron-dense lysosomes. However, the BMDCs treated with the 10^{-12}M MENK plus 1.1 μg/ml PTD for 48 h were matured with irregular in shape and displayed many dendritic cytoplasmic protrusions with varying width. The nuclei were dark with clumps of chromatin beneath the nuclear envelope throughout the nucleoplasm. Numerous organelles, such as rich mitochondria, well developed rough reticulum, were observed in the cytoplasm and around the nuclei (**Fig. 5**).

Morphology under SEM. Further morphological observation under SEM revealed that BMDCs had a variety of cell shapes such as bipolar elongated cells and elaborated stellate cells. The BMDCs showed small round shaped with less body extensions in the RPMI 1640 group. After treated with 10^{-12}M MENK plus 1.1 μg/ml PTD for 48 h, the BMDCs showed several fine dendrites, radiating from the cell body (×2000). Most pseudopods were

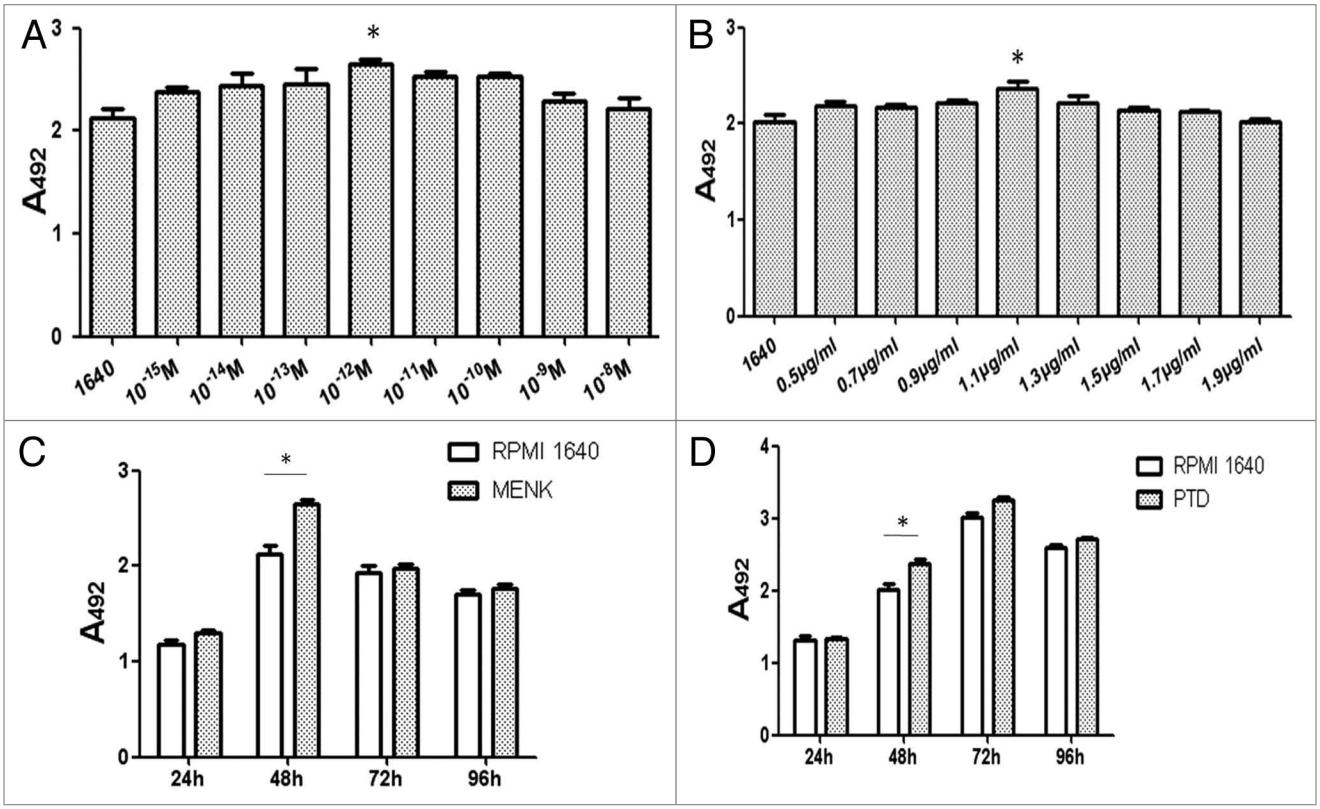

Figure 2. BMDCs were treated with 10^{-15}M to 10^{-8}M MENK and 0.5 μg/ml to 1.9 μg/ml PTD respectively for 48 h. OD was recorded at 492 nm and all data were represented as the means ± SEM (n = 3) and optimal concentrations for both MENK and PTD were obtained (**Fig. 2A and B**).

long and uniform in width with blunt terminations, but smaller spinous processes were also evident (**Fig. 6**).

Flow cytometry analysis of BMDC phenotypes. The BMDCs cultured for 7 d with GM-CSF plus IL-4 were incubated in the presence of different drugs. The comparative phenotypic analysis was performed by FACS. BMDCs treated with 10^{-12}M MENK plus 1.1 μg/ml PTD for 48h evidently upregulated the frequency of expressed key surface markers (e.g., CD40, CD80, CD83, CD86 and MHC-II), when compared with those in the RPMI 1640 group, the MENK group or the PTD group (**Fig. 7**). However, the expression level and the MFI of CD40 on the BMDCs were not very significant. Concretely, the percentage of CD80 molecules yielded 59.97 ± 8.37% in the testing group ($p < 0.01$) versus 19.99 ± 2.39% in the RPMI 1640 group, and ($p < 0.05$) vs. 47.99 ± 2.06% or 44.75 ± 1.44% in MENK group or PTD group. The percentage of the CD40 molecules yielded 48.77 ± 1.60% in the testing group ($p < 0.01$) vs. 15.52 ± 2.28% in the RPMI 1640 group, and vs. 39.28 ± 0.74% or 36.64 ± 2.19% in MENK group or PTD group ($p < 0.05$). The percentage of the CD83 molecules yielded 53.01 ± 1.28% in the testing group ($p < 0.01$) vs. 13.19 ± 1.97% in the RPMI 1640 group, and vs. 42.89 ± 3.06% or 40.38 ± 1.89% in MENK group or PTD group ($p < 0.05$). The percentage of the CD86 molecules yielded 46.54 ± 1.01% in the testing group ($p < 0.01$) versus 18.51 ± 1.35% in the RPMI 1640 control group, and vs. 36.49 ± 0.73% or 34.78 ± 1.45% in MENK group or PTD group ($p < 0.05$). The percentage of MHC-II molecules yielded 61.68 ± 1.81%

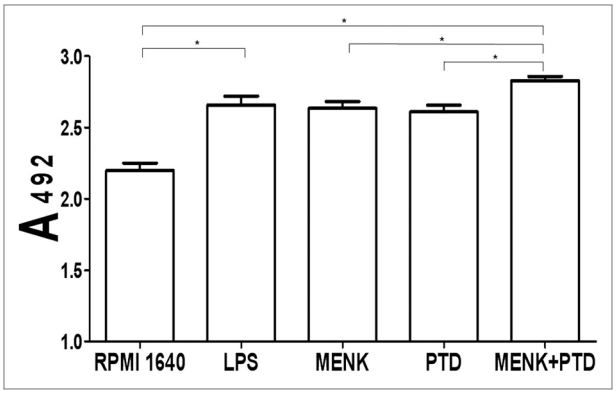

Figure 3. BMDC proliferation after treatment with 10^{-12}M MENK plus 1.1 μg/ml PTD for 48 h. The proliferation of BMDCs after treatment with LPS or 10^{-12}M MENK plus 1.1 μg/ml PTD for 48 h increased significantly (*$p < 0.05$, **$p < 0.01$). The data shown were means of three independent experiments ± SEM.

in the testing group ($p < 0.01$) vs. 29.23 ± 3.28% in the RPMI 1640 control group, and vs. 51.26 ± 1.48% or 51.26 ± 1.71% in MENK group or PTD group ($p < 0.05$).

Cellular immunohistochemistry for phagocytosis by murine BMDCs. The endocytic capacity of mice BMDCs was downregulated during maturation. The immature BMDCs were highly endocytic compared with mature BMDCs as reflected by the

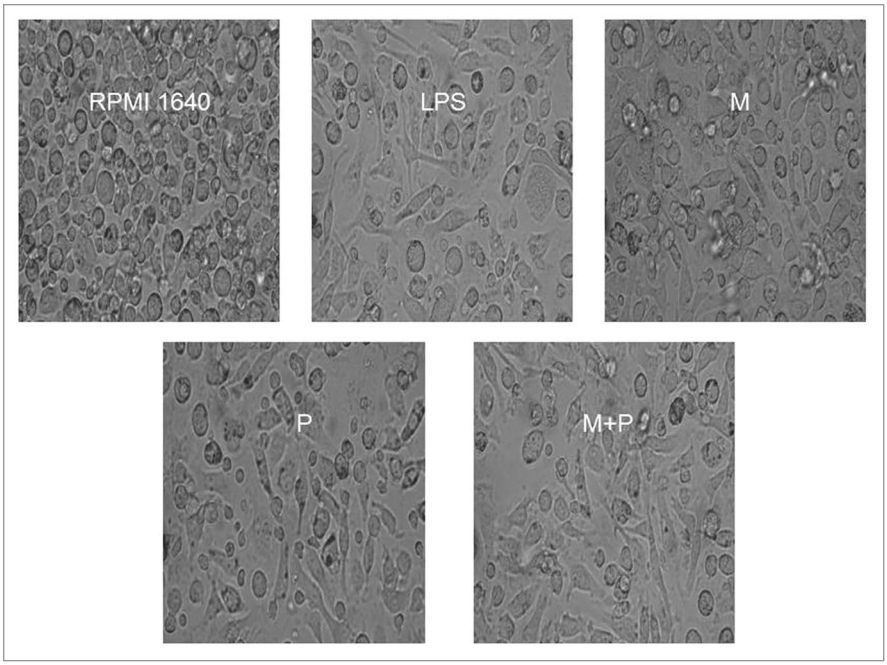

Figure 4. The purified BMDCs, treated with LPS, 10^{-12}M MENK(M), 1.1 μg/ml PTD(P) and 10^{-12}M MENK plus 1.1 μg/ml PTD(M+P) for 48 h, were observed under Inverted Phase Contrast Microscope (×200).

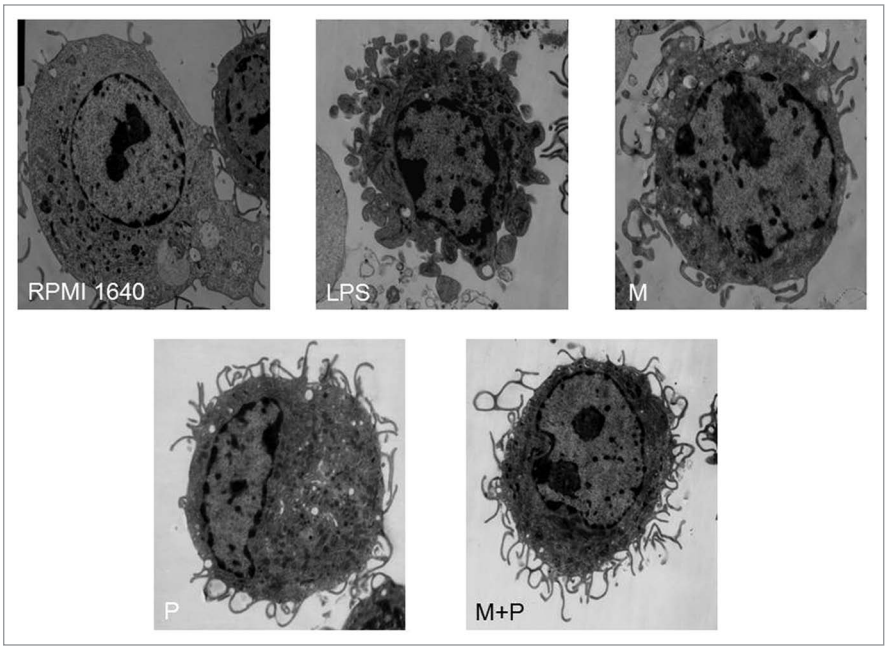

Figure 5. Morphology of BMDCs after incubated for 48h were observed under TEM (×5000). The images revealed smooth reticulum, vacuoles and more lysosomal or phagocytic structure of BMDCs in the 1640 group. However, BMDCs in the testing group displayed a rather dark cytoplasm with long and slender cellular processes. Also the cytoplasm contained free ribosomes, cisternae of endoplasmic reticulum, and a prominent Golgi apparatus.

photos which showed pinocytosis of horseradish peroxidase in process with the difference in staining intensity between the different groups compared at the same time points. The DAB-labeled precipitation in the RPMI 1640 group was well defined (**Fig. 8**). However, less DAB precipitate was found in BMDCs treated with 10^{-12}M MENK plus 1.1 μg/ml PTD for 48 h.

Quantitation of endocytosis by FACS. The transition of BMDCs from an immature to a more mature stage was associated with a decrease in ability to phagocyte antigens. To our expectation, flow cytometry analysis revealed that drug-treated BMDCs significantly diminished their endocytic activities and results correlated well with their maturational status. The immature BMDCs with highly endocytic activity, when treated with 10^{-12}M MENK plus 1.1 μg/ml PTD for 48h, could apparently decrease uptake of FITC-dextran. A summary of three experiments was shown in **Figure 9**. Concretely, the percentage of FITC-dextran particles taken by BMDCs decreased from 66.06 ± 4.48% to 42.98 ± 2.61% 10^{-12} in M MENK plus 1.1 μg/ml PTD group.

Biochemical analysis of ACP activity. To assess the endocytic capacity of BMDCs, biochemical analysis of ACP activity was performed. Differences were evident between control and testing groups. This is to say, after treatment with the 10^{-12}M MENK plus 1.1 μg/ml PTD for 48 h, the immature BMDCs became more mature with a marked decrease in ACP activity, indicating a gradual termination of phagocytosis or antigen ingestion (**Fig. 10**). ACP activity of the BMDCs was measured by the method illustrated above and yielded the following activity numbers: 36.60 ± 3.62 U/gprot in the testing group vs. 60.81 ± 0.71 U/gprot in the RPMI 1640 group ($p < 0.01$), vs. 44.70 ± 4.08 U/gprot or 45.87 ± 1.37 U/gprot in MENK group or PTD group ($p < 0.05$).

Cytokine assay by ELISA. After incubation with different drugs for 48 h, the cell-free supernatants were collected and IL-12p70 and TNF-α were measured by sandwich ELISA. The results were representative of two experiments performed separately in triplicate (*$p < 0.05$, **$p < 0.01$) (**Fig. 11**). Upon maturation, higher levels of IL-12 were secreted at concentrations of 41.37 ± 4.22 pg/ml in the testing group vs. 18.48 ± 3.37 pg/ml of IL-12 produced in the RPMI 1640 group ($p < 0.01$), and vs. 27.31 ± 1.12 pg/ml or 26.69 ± 0.43 pg/ml in MENK group or PTD group ($p < 0.05$). TNF-α was detected out at concentrations of 60.08 ± 9.26 pg/ml ($p < 0.01$) in the testing group

vs. 18.33 ± 3.83 pg/ml of TNF-α produced in the RPMI 1640 group, and vs. 35.44 ± 1.77 pg/ml or 34.00 ± 3.46 pg/ml in MENK group or PTD group ($p < 0.05$).

Mixed lymphocyte reaction (MLR). The mature BMDCs usually have potential to drive T-cell activation. The ratios of dendritic cells to T cells of 1:1, 1:5, 1:10, 1:50 and 1:100, respectively were used in this test. The results reflected that when the ratio of BMDCs to T cells was at 1:1 the BMDCs treated with 10^{-12}M MENK plus 1.1 μg/ml PTD for 48 h showed a significant ability in driving T lymphocytes activation and proliferation. OD492 nm yielded 0.87 ± 0.03 in mature BMDCs treated by the MENK plus PTD vs. 0.47 ± 0.01 in immature BMDCs without treatment ($p < 0.01$) (**Fig. 12**).

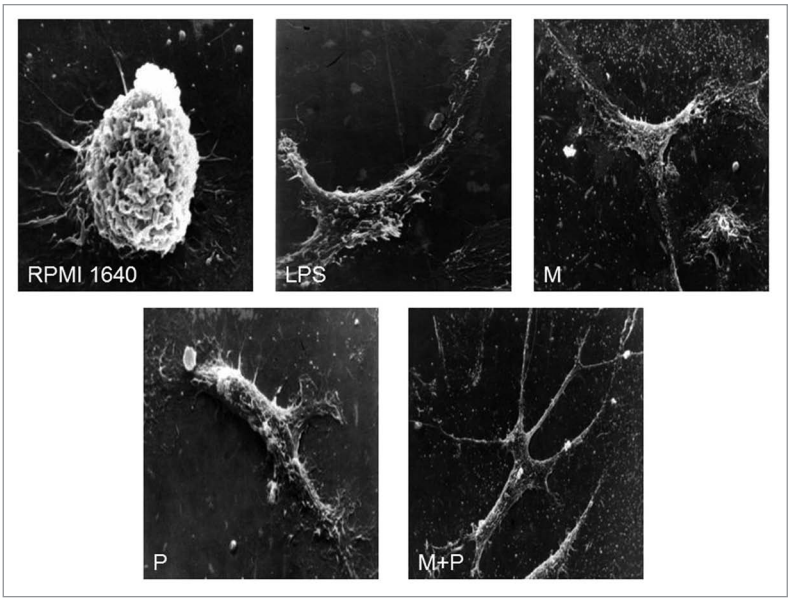

Figure 6. Morphology of BMDCs after incubated for 48h were observed under SEM (RPMI 1640: ×5000; LPS, M, P and M+P: ×2000).

Discussion

Endogenous opioid peptides serve to regulate the growth of developing, neoplastic, renew and heal tissues, and function in both prokaryotes and eukaryotes.[28,29] One native opioid peptide, MENK, has emerged as a modulator on several immunological functions both in vitro and in vivo such as enhancing the proliferation of peripheral blood lymphocytes and splenocytes.[30] MENK possesses bilateral regulation on immune cells, which means that MENK at higher concentrations such as 10^{-6}M or lower concentrations such as 10^{-18}M will delay immune cell growth and the possible mechanism is MENK can interact with OGFr to upregulate cyclin-dependent kinase inhibitory (CKI) pathways and markedly delay the G_1/S phase of the cell cycle.[31-34] However, MENK at a range of physiological concentrations between 10^{-11} and 10^{-15}M will enhance immune cell growth. Beyond the well-known interaction of MENK with the μ- and δ-opioid receptor, the peptide has been shown to bind with a distinct receptor-type, named zeta (ζ) receptors.[35] Because zeta receptors were found to be involved in the regulation of cell growth by the "opioid growth factor" (OGF) MENK. Recently, scientists have identified a novel endogenous opioid system (OGF-OGFr) that inhibited cell proliferation, migration, angiogenesis, and tissue organization.[31,34,36-39] Our previous work has proven that MENK could intensify in the DC-CD4+T cell pathway, stimulate proliferation of lymphocytes in human peripheral blood, induce DC progenitors to develop to mDC, and drive macrophage polarization into M1-type in mice bearing tumor.[27,40-42]

PTD, a synthetic substance, has been shown to ameliorate different functions of innate and adaptive immune responses both in animals and humans.[28] It has been reported that PTD was able to enhance the effectors of the innate immunity responses by potentiating different functions of the professional phagocytes and NK cell activity; PTD also significantly increased the proliferation of spleen cells in response to Con-A and interleukin-2 (IL-2) stimulation.[28,43] On the other hand, large clinical trials have been conducted on patients shown that PTD displayed a beneficial activity in recurrent upper respiratory and urinary tract infections in children, both in the acute phase and in the prevention of the relapses.[44-47]

In this study we analyzed the effect of the combined treatment with MENK and PTD on BMDC maturation. As a result, the BMDCs have been undergone a complex maturation process from antigen-capturing cells into antigen-presenting cells in response to the synergistic effect of MENK and PTD treatment. Our major findings were as evidenced as: (1) When treated with 10^{-12}M MENK plus 1.1 μg/ml PTD for 48 h, the number of BMDCs could remarkably increase and show more maturation than those treated with either MENK or PTD alone; (2) The co-stimulatory molecules CD80, CD86, CD40, followed by antigen-presenting molecules MHC-II and CD83, increased significantly. However, there was no statistically significant difference of the BMDC phenotype for 24 h. The authors[27] in my group showed that a 24 h-incubation of DC2.4 cell line with MENK alone did induce significantly higher expression of maturational surface markers. This was due to the use of established cell line; (3) FITC–dextran uptaking and ACP testing were used to evaluate the antigen-uptake capability, which is characteristic of immature DCs.The addition of 10^{-12}M MENK plus 1.1 μg/ml PTD to the BMDC cultures decreased the number of DAB precipitation and the content of ACP, indicating lowering of the antigen uptaking capability; (4) Both phenotypic and functional findings were in concert with higher expression of IL-12 and TNF-α and promote the proliferation of lymphocytes. The improved efficacy of DC vaccines in mice, suggested the significance of IL-12 in augmenting CTL-mediated cytotoxicity. The production of IL-12 and TNF-α, which were cytokines associated with the differentiation of Th1 cells positioned downstream from DCs, was augmented by the addition of 10^{-12}M MENK plus 1.1 μg/ml PTD. All these results indicated that combined treatment with MENK and PTD has an

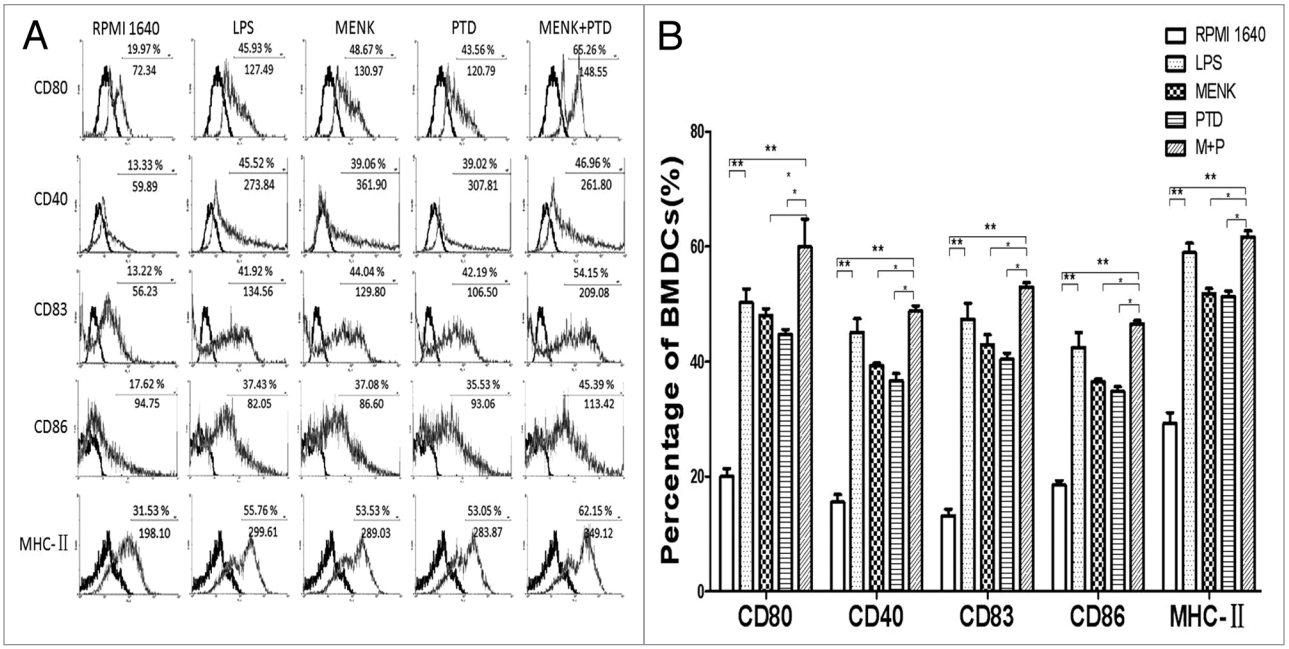

Figure 7. FACS analysis of BMDCs treated with MENK plus PTD for 48 h. (**A**) The percentagesin the plot indicated the BMDCs number and below them the digits represent mean fluorescence intensity. Representative FACS plots of three independent experiments. The bold line histograms show the background staining with isotype control mAbs, and thin line histograms represent specific staining of the indicated cell surface markers. Statistical summary of these were shown as means ± S.E.M. (n = 3). (*p < 0.05, **p < 0.01) (**B**).

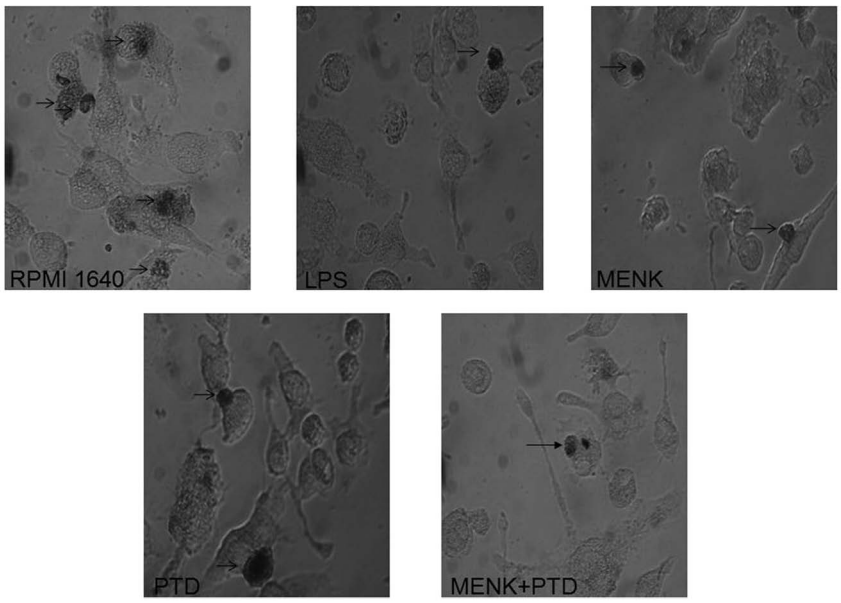

Figure 8. BMDCs treated with 10^{-12}M MENK plus 1.1 μg/ml PTD for 48 h were stained with DAB kit and observed under an Inverted Phase Contrast Microscope. Black arrows pointed brown staining. (×400)

immunostimulatory effect in a synergistic manner on the maturation of BMDCs.

Activation and maturation of DCs has a pivotal impact on immune response. Most experimental adjuvants provide signals to which the innate immune system vigorously reacts, resulting in a generalized potentiation of the immune system so that the Ag co-administered with adjuvant can be taken up more effectively, processed and presented by activated DCs. Dendritic cells are known to be the most professional APCs with a pivotal role in both immunity induction and antigen capture, processing and presentation, and express co-stimulation signals that activate T lymphocytes and NK cells.[47-50] DC-based treatment strategies are increasingly recognized to have therapeutic potential in many immunopathological conditions including cancer, autoimmunity, and allogeneic transplantation.[51-57]

Early experiments had indicated that MENK acted as a novel biological treatment for advanced pancreatic cancer, colorectal cancer,[58] human hepatocellular cancer,[59] thyroid follicular cell-derived cancers,[60] and inhibits the progression of human squamous cell carcinoma of the head and neck transplanted into nude mice.[61] Moreover, PTD could stimulate the proliferation of human PBMCs from neoplastic donors. These findings reflected the ability of PTD to restore some parameters of immune responses.[62] Preclinical studies have already shown that the combination of MENK with PTD biotherapy with conventional care (e.g., gemcitabine) has even greater efficacy and reduces the toxicity of chemotherapy.[63] Certainly, the

combination of MENK with PTD needs to be investigated in the clinical setting. If these beneficial effects would be confirmed in further studies, it could be attributed to the fact that the combined action of MENK and PTD probably increases immunity and natural defense. Along with advances in tumor immunology now becoming a topic of interest, high expectations have been directed toward DCs, which are potent APCs and the development of DC therapy is being researched by many investigators. One of the noted DC therapies is DC vaccine therapy, which means that tumor antigen-loaded DC might potentially add therapeutic benefit with DC-based vaccination. Only immature DC can provide uptake and processing of tumor-derived protein or tumor lysate, which is of major importance for tumor vaccine generation. Although DC vaccine therapy continues to attract attention as a new immunotherapy, many clinical results are still less than satisfactory because of an accentuated immune-escape mechanism in the cancer-bearing host and the failure of cultured DCs to mature, resulting in the failure of T-cell responses. Mature DCs can be used as vaccines after in vitro tumor peptide loading or after their immature DC precursors were initially loaded with tumor protein or lysate and matured thereafter.[64-68] To resolve this problem, immunomodulatory combined action of MENK and PTD on DCs was detected in this study. The results indicated that the combination of MENK with PTD induced morphological, phenotypic and functional maturation of DCs derived from mouse bone marrow cells. Our previous studies have proven that PTD or MENK alone could induce the maturation of murine DCs.[27] Furthermore, there are often additional benefits when these therapeutics are used in combination, rather than separately.

Despite the fruitful data that we have obtained, there is still leaving much to be investigated, such as the concrete working mechanisms of MENK combined with PTD on BMDC at signal level and clinical significance of this combinational method. Of course, such studies require large numbers of patients and long follow-up periods to determine the impact of the combination of MENK with PTD on disease-free and overall survival. Thus, more work is required to see the results. Ultimately, the use of biological therapies to treat the cause rather than the symptoms introduces an entirely new chapter in benefiting patients with devastating disease. Meanwhile, we may consider the use of MENK in combination with other known inducers to DC as a future direction.

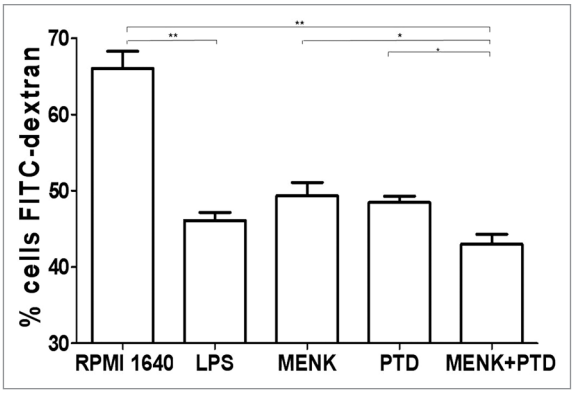

Figure 9. FITC-dextran uptaking experiments were performed. The treated BMDCs were suspended in RPMI 1640, incubated with 1 mg/ml of FITC-dextran for 1h at 37°C or 4°C, and then used in uptake experiments. The quantitative uptake of FITC-dextran by the BMDCs was determined by the FACS analysis. Each data point represent the mean ± SEM (n = 3) (*p < 0.05, **p < 0.01).

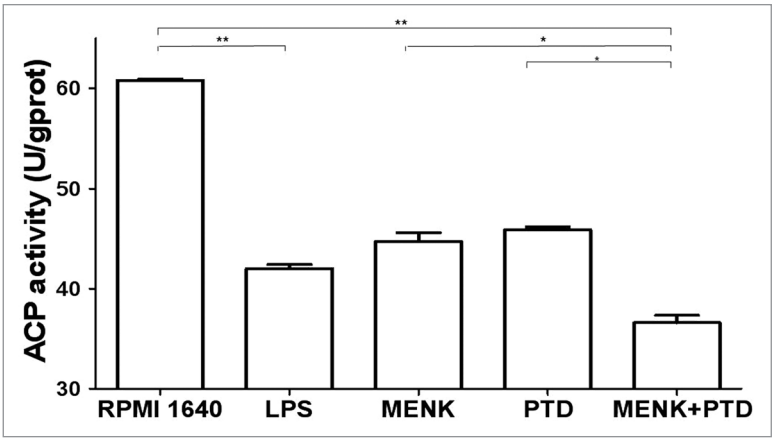

Figure 10. ACP activity was measured by ACP testing kit. Downregulation of ACP activity represents maturation of BMDCs as losing phagocytosis. All data were expressed as mean ± SEM (n = 3) (*p < 0.05, **p < 0.01).

Materials and Methods

Key reagents. MENK was obtained from Penta Biotech Inc. USA (≥ 97 purity). PTD (> 99% purity) was a gift from Sunstone Pharmaceutical Company. The mAbs used in this study were purchased from eBioscience and BD PharMingen respectively. IL-4 (Catalog number: 315–03) and GM-CSF (Catalog number: 214-14) were obtained from PeproTech Inc. The ELISA assay kits for IL-12p70 and TNF-α analysis were purchased from eBioscience. LPS (Catalog number: L-2880, 10 ng/ml was used) as a positive control was a product of Sigma-Aldrich. MACS (MiltenyiBiotec). Other chemicals frequently used in our laboratory were all products from Sigma-Aldrich or BD PharMingen.

Mice. Female 4–6 week-old C57BL/6 mice were obtained from China Medical University and allowed to acclimatize for at least one week in our facility before use. The mice were maintained under pathogen-free conditions and handled according to international guidelines.

Generation and purification of BMDCs. After sacrificing mice, all muscle tissues from the femurs and tibias were removed with gauze. Intact bones were placed in a 60-mm dish with 75% ethanol for 2 min for disinfection, washed twice with ice-cold PBS, and transferred into a fresh dish with RPMI 1640. Both ends of the bones were cut with scissors in the dish, and then the marrow was flushed out using 1ml RPMI 1640 with a 1ml syringe. The bone marrow cells were suspended and treated with RBC lysis (155 mM NH_4Cl, 10 mM $NaHCO_3$, 0.1 mM EDTA).

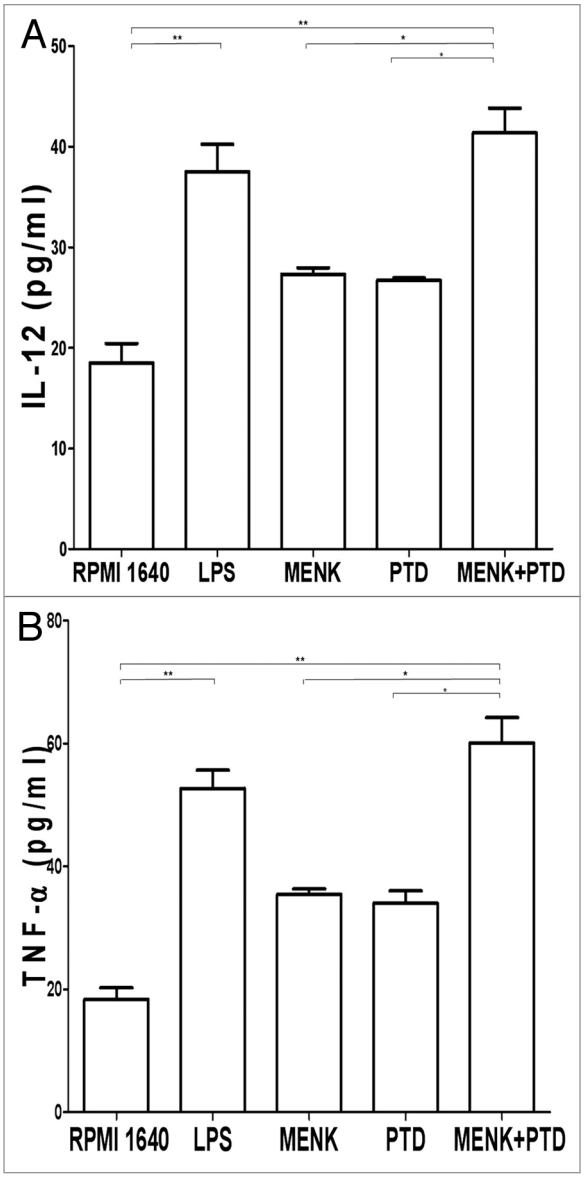

Figure 11. Supernatants of BMDC cultures were harvested 48h later for IL-12 (**Fig. 11A**) and TNF-α (**Fig. 11B**) per manufacturer's protocol. Optical densities at 492 mm were measured using an iMark Microplate Reader. The results were representative of two experiments performed separately in triplicate (*p < 0.05, **p < 0.01).

Viable cells were counted using a Neubauer chamber and trypan blue exclusion. Then cells were plated in six-well culture plates (10^6 cells/ml, 3ml/well) in RPMI 1640 medium supplemented with penicillin (100 U/ml, Sigma) streptomycin (100 mg/ml, Sigma), L-glutamine (2 mM, Sigma), 2-mercaptoethanol (50 mM, Sigma) and 10% heat-inactivated fetal bovine serum (FBS), 10 ng/ml recombinant murine GM-CSF and 10 ng/ml IL-4. At day 0, 2, 4 and 6 of culture, floating cells were gently removed, and fresh medium was added. At day 7 of culture, non-adherent cells and loosely adherent proliferating DC aggregates were collected and purified by magnetic cell sorting using the CD11c positive selection kit and MACS columns (MiltebyiBiotec). The purity of BMDCs was > 95% as determined by CD11c staining. The gating strategy employed for data analysis was to restrict the analysis to live singlets of CD11c-positive cells. Then the cells were counted, seeded and cultivated in tissue culture plates 12 h before any further experimental procedure.[69]

Proliferation assays. The MTS/PMS assay was initiated as follows: BMDCs were seeded in a 96-well culture plate using 2 × 10^4 cells/well (n = 3) in 100 μl culture medium. Added 100 μl MENK or PTD in concentration range from 10^{-15}M to 10^{-8}M (0.5 μg/ml to 1.9 μg/ml, respectively). After incubation at 37°C in a humidified incubator with 5% CO_2, the untreated and treated BMDCs were exposed in conjunction with 20μl MTS/PMS mixture (final concentrations: MTS, 240 pg/ml; PMS, 2.4 pg/ml) and cultured for 4 h. The optimal concentration and time point were measured calorimetrically by the MTS assay, and the optical density was read by iMarkMicroplate Reader (BIO-BAD) at 492 nm.

When the best concentration and time points were identified, further experiments were also made by the MTS assay to identify the synergistic immunostimulatory effect of MENK and PTD on the murine BMDCs.

Morphology under light microscopy. The purified BMDCs, treated with RPMI 1640, LPS, 10^{-12}M MENK (M), 1.1 μg/ml PTD (P), and 10^{-12}M MENK plus 1.1 μg/ml PTD for 48 h, were observed under Inverted Phase Contrast Microscope (CMS GmbH Light Microscopes, Leica Microsystems).

Morphology under TEM. After treatment, BMDCs were pelleted, re-suspended in 0.5 ml PBS 0.05M, pH 7.2 and fixed overnight in 2.5% glutaraldehyde, followed by 1% osmium teroxide, dehydrated in ethanol and embedded in epon. Sections were cut on a Reiehert-Jung Ultracut E, stained with uranyl acetate and lead citrate and examined in a transmission electron microscopy (JEOL JEM-1200EX). The TEM was operated at an 80–100kV accelerating voltage.

Morphology under SEM. All samples were fixed with 2.5% glutaraldehyde and 4% paraformaldehyde in phosphate buffer (pH 7.4) for 1h at room temperature. Then cells were post-fixed 1h with 2% osmium tetroxide solution for 30 min at 4°C. Following each fixation, samples were washed twice in PBS containing BSA, dehydrated in graded ethanol, and dried at critical point in liquid CO_2 under 95-bar pressure. Then coverslips were cold-sputted coated with gold and observed in a JECL JSM-T300 scanning electron microscopy.

Flow cytometry analysis of BMDC phenotypes. After 48h of culture in the presence or absence of LPS, MENK/PTD or both, cells were washed twice with PBS containing 3% FBS at 300 g for 5 min and re-suspended in the same buffer. Surface phenotypes of BMDCs were analyzed, and then cells were incubated with 10 μl anti-CD40 FITC, anti-CD86 PE, anti-CD80 FITC, anti-CD83 FITC and anti-MHCII PE antibodies or isotype-matched (goat anti-mouse antibodies, coupled to FITC or PE) negative control mAbs respectively at the same concentration for 30 min at 4°C for optimal staining. Each incubation was followed by two washing steps without a live/dead cell stain. The staining cells were fixed prior to analysis, and then run on an FACS Calibur (Becton Dickinson) flowcytometer, and data were analyzed with WinMDI2.9 (Joseph Trotter, BD Biosciences).

The percentages of positive cells and mean fluorescence intensities (MFI) were calculated. The gating strategy employed for data analysis was to restrict the analysis to live singlets of CD40, CD86, CD80, CD83 or MHCII-positive cells. The volume of mAb was optimized in preliminary experiments.

Cellular immunohistochemistry for phagocytosis by murine BMDCs. BMDCs (10^5 ml), treated with LPS, MENK, PTD or 10^{-12}M MENK plus 1.1 μg/ml PTD for 48 h, were incubated with rabbit anti-mouse IgG labeled with horseradish peroxidase and then fixed with methanol for 4 h, followed by staining with DAB Kit. Sections were observed under an Inverted Phase Contrast Microscope (CMS GmbH Light Microscopes, Leica Microsystems).

Quantitation of endocytosis by FACS. After 48h stimulation, the BMDCs were washed three times and incubated for 1h with a final concentration of 1 mg/ml of FITC-dextran (M_r = 40,000; Sigma) at 37°C, subsequently at 4°C for 1 h. After incubation, the cells were washed twice in PBS to remove excess dextran. The quantitative uptake of FITC-dextran by the BMDCs was determined by the FACS analysis.

Biochemical analysis of ACP activity. The ACP activity of the experimental BMDCs was measured at OD520 nm by the phenol-4-APP (amino antipyrine) method in conjunction with ACP testing kit.

Protein concentration in each fraction was measured by the method of Lowry et al. using BSA as standard.

Cytokine assay by ELISA. To measure cytokine levels in the supernatants of DCs, BMDCs (5 μ × 10^4 /well) were stimulated with indicated concentrations of LPS, MENK, PTD or 10^{-12}M MENK plus 1.1 μg/ml PTD for 48h. The culture medium was harvested and the concentrations of mouse IL-12 and TNF-α were measured using the respective, commercially available ELISA kit according to the manufacturer's protocols. Readings were made at 450 nm with correction at 570 nm, on the iMark Microplate Reader (BIO-RAD).

Mixed lymphocyte reaction (MLR). In order to test whether the MENK plus PTD-stimulated BMDCs can activate T cell proliferation, BMDCs from C57BL/6 mice were treated with LPS, MENK, PTD, the MENK plus PTD or left untreated for 48 h. At 3 d, the BMDCs were collected and washed three times with RPMI 1640, and finally the cells number was adjusted to 3 × 10^5 ml to serve as stimulating cells. Lymphocytes were isolated from the spleen of C57BL/6 mice to serve as responding cells. The lymphocytes (3 × 10^7 ml) were incubated in flat-bottomed 96-well plates (Corning-Costar) with graded numbers of BMDCs (at a ratio of 1:1, 10:1, 50:1 and 100:1). After incubation for three days, cell activation and proliferation was evaluated using the MTS assay, and the absorbance was read at 492 nm using the bichromatic microplate reader according to the manufacturer's instructions. Results were expressed as the mean ± SEM from triplicate wells.

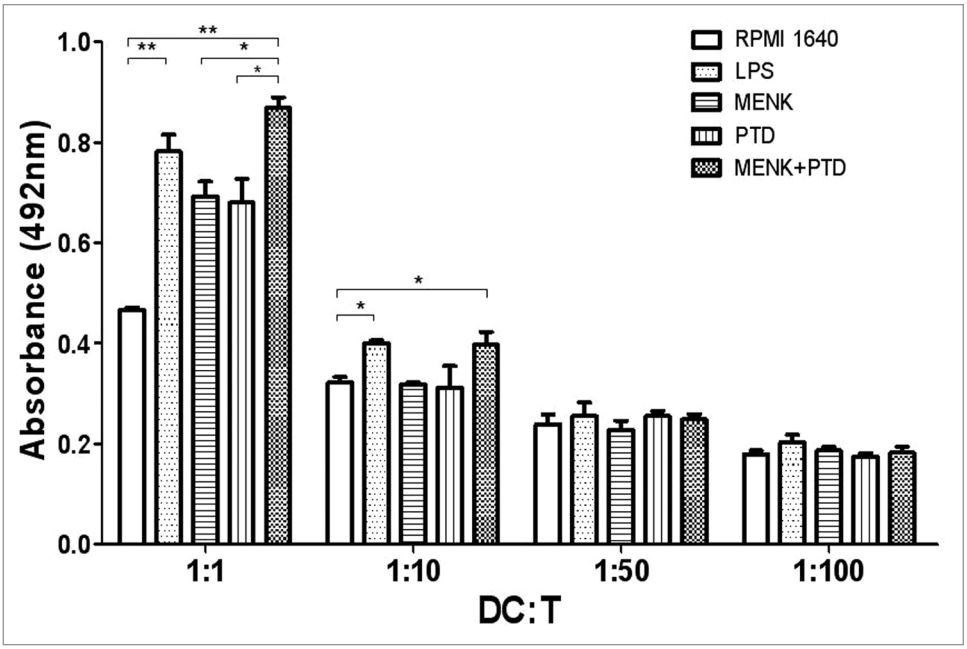

Figure 12. Test of BMDC-driven T lymphocytes. The T lymphocytes proliferation reflected the ability of matured BMDCs to initiate T cell response. The lymphocytes (3 × 10^7/ml) were incubated in flat-bottomed 96-well plates (Corning-Costar) with graded numbers of BMDCs (at a ratio of 1:1, 10:1, 50:1 and 100:1). After incubation for three days, cell activation and proliferation was evaluated using the MTS assay, and the absorbance was read at 492 nm using the bichromatic microplate reader according to the manufacturer's instructions. The results were representative of two experiments performed separately in triplicate (*$p < 0.05$, **$p < 0.01$).

Data and statistical analysis. Results were given as mean ± S.E.M. The Statistical Package for Social Sciences 13.0 software (SPSS) was used for statistical analyses including one-way ANOVA and Student's t-test. A probability (P)-value < 0.05 was considered statistically significant. All the figures of this study were made by GraphPad Prism 5.01 software (GraphPad Software Inc.).

Disclosure of Potential Conflicts of Interest

No potential conflicts of interest were disclosed.

Acknowledgments

This work was supported financially by China Liaoning provincial foundation, No.2006305007, 2012225016 (to F.S.).

References

1. Hughes J, Smith TW, Kosterlitz HW, Fothergill LA, Morgan BA, Morris HR. Identification of two related pentapeptides from the brain with potent opiate agonist activity. Nature 1975; 258:577-80; PMID:1207728; http://dx.doi.org/10.1038/258577a0.
2. Zagon IS, Donahue RN, Bonneau RH, McLaughlin PJ. B lymphocyte proliferation is suppressed by the opioid growth factor-opioid growth factor receptor axis: Implication for the treatment of autoimmune diseases. Immunobiology 2011; 216:173-83; PMID:20598772; http://dx.doi.org/10.1016/j.imbio.2010.06.001.
3. Bodnar RJ. Endogenous opiates and behavior: 2008. Peptides 2009; 30:2432-79; PMID:19793543; http://dx.doi.org/10.1016/j.peptides.2009.09.027.
4. Bodnar RJ. Endogenous opiates and behavior: 2010. Peptides 2011; 32:2522-52; PMID:21983105; http://dx.doi.org/10.1016/j.peptides.2011.09.020.
5. Akil H, Watson SJ, Young E, Lewis ME, Khachaturian H, Walker JM. Endogenous opioids: biology and function. Annu Rev Neurosci 1984; 7:223-55; PMID:6324644; http://dx.doi.org/10.1146/annurev.ne.07.030184.001255.
6. Sharma HS. Interaction between amino acid neurotransmitters and opioid receptors in hyperthermia-induced brain pathology. Prog Brain Res 2007; 162:295-317; PMID:17645925; http://dx.doi.org/10.1016/S0079-6123(06)62015-3.
7. Deroee AF, Nezami BG, Mehr SE, Hosseini R, Salmasi AH, Talab SS, et al.; Armin FarajzadehDeroee. Cholestasis induced nephrotoxicity: the role of endogenous opioids. Life Sci 2010; 86:488-92; PMID:20153756; http://dx.doi.org/10.1016/j.lfs.2010.02.005.
8. Plow EB, Pascual-Leone A, Machado A. Brain stimulation in the treatment of chronic neuropathic and non-cancerous pain. J Pain 2012; 13:411-24; PMID:22484179; http://dx.doi.org/10.1016/j.jpain.2012.02.001.
9. Kishori B, Reddy PS. Role of methionine-enkephalin on the regulation of carbohydrate metabolism in the rice field crab Oziotelphusa senex senex. C R Biol 2005; 328:812-20; PMID:16168362; http://dx.doi.org/10.1016/j.crvi.2005.07.001.
10. Pellizzari EH, Barontini M, Figuerola MdeL, Cigorraga SB, Levin G. Possible autocrine enkephalin regulation of catecholamine release in human pheochromocytoma cells. Life Sci 2008; 83:413-20; PMID:18706432; http://dx.doi.org/10.1016/j.lfs.2008.07.004.
11. McLaughlin PJ, Keiper CL, Verderame MF, Zagon IS. Targeted overexpression of OGFr in epithelium of transgenic mice suppresses cell proliferation and impairs full-thickness wound closure. Am J Physiol Regul Integr Comp Physiol 2012; 302:R1084-90; PMID:22338080; http://dx.doi.org/10.1152/ajpregu.00670.2011.
12. Donahue RN, McLaughlin PJ, Zagon IS. Underexpression of the opioid growth factor receptor promotes progression of human ovarian cancer. Exp Biol Med (Maywood) 2012; 237:167-77; PMID:22328595; http://dx.doi.org/10.1258/ebm.2011.011321.
13. Fanning J, Hossler CA, Kesterson JP, Donahue RN, McLaughlin PJ, Zagon IS. Expression of the opioid growth factor-opioid growth factor receptor axis in human ovarian cancer. Gynecol Oncol 2012; 124:319-24; PMID:22037317; http://dx.doi.org/10.1016/j.ygyno.2011.10.024.
14. Donahue RN, McLaughlin PJ, Zagon IS. Low-dose naltrexone targets the opioid growth factor-opioid growth factor receptor pathway to inhibit cell proliferation: mechanistic evidence from a tissue culture model. Exp Biol Med (Maywood) 2011; 236:1036-50; PMID:21807817; http://dx.doi.org/10.1258/ebm.2011.011121.
15. Lou HG, Ruan ZR, Jiang B. Quantitative determination of pidotimod in human plasma by liquid chromatography tandem mass spectrometry: application to a bioequivalence study. Arzneimittelforschung 2012; 62:99-104; PMID:22344555; http://dx.doi.org/10.1055/s-0031-1297983.
16. Riboldi P, Gerosa M, Meroni PL. Pidotimod: a reappraisal. Int J Immunopathol Pharmacol 2009; 22:255-62; PMID:19505378.
17. Masihi KN. Immunomodulatory agents for prophylaxis and therapy of infections. Int J Antimicrob Agents 2000; 14:181-91; PMID:10773486; http://dx.doi.org/10.1016/S0924-8579(99)00161-2.
18. La Mantia I, Grillo C, Mattina T, Zaccone P, Xiang M, Di Mauro M, et al. Prophylaxis with the novel immunomodulator pidotimod reduces the frequency and severity of upper respiratory tract infections in children with Down's syndrome. J Chemother 1999; 11:126-30; PMID:10326743.
19. Aivazis V, Hatzimichail A, Papachristou A, Valeri R, Iuga-Donca G. Clinical evaluation and changes of the respiratory epithelium function after administration of Pidotimod in Greek children with recurrent respiratory tract infections. Minerva Pediatr 2002; 54:315-9; PMID:12131867.
20. Van Nuffel AM, Tuyaerts S, Benteyn D, Wilgenhof S, Corthals J, Heirman C, et al. Epitope and HLA-type independent monitoring of antigen-specific T-cells after treatment with dendritic cells presenting full-length tumor antigens. J Immunol Methods 2012; 377:23-36; PMID:22269772; http://dx.doi.org/10.1016/j.jim.2011.12.010.
21. Crispin JC, Alcocer-Varela J. The role myeloid dendritic cells play in the pathogenesis of systemic lupus erythematosus. Autoimmun Rev 2007; 6:450-6; PMID:17643932; http://dx.doi.org/10.1016/j.autrev.2007.01.014.
22. Saha A, Chatterjee SK. Dendritic cells pulsed with an anti-idiotype antibody mimicking Her-2/neu induced protective antitumor immunity in two lines of Her-2/neu transgenic mice. Cell Immunol 2010; 263:9-21; PMID:20236626; http://dx.doi.org/10.1016/j.cellimm.2010.02.010.
23. Moser JM, Sassano ER, Leistritz C, Eatrides JM, Phogat S, Koff W, et al. Optimization of a dendritic cell-based assay for the in vitro priming of naïve human CD4+ T cells. J Immunol Methods 2010; 353:8-19; PMID:19925804; http://dx.doi.org/10.1016/j.jim.2009.11.006.
24. Hargadon KM, Forrest OA, Reddy PR. Suppression of the maturation and activation of the dendritic cell line DC2.4 by melanoma-derived factors. Cell Immunol 2012; 272:275-82; PMID:22051048; http://dx.doi.org/10.1016/j.cellimm.2011.10.003.
25. Trepiakas R, Pedersen AE, Met Ö, Svane IM. Addition of interferon-alpha to a standard maturation cocktail induces CD38 up-regulation and increases dendritic cell function. Vaccine 2009; 27:2213-9; PMID:19428835; http://dx.doi.org/10.1016/j.vaccine.2009.02.015.
26. Giagulli C, Noerder M, Avolio M, Becker PD, Fiorentini S, Guzman CA, et al. Pidotimod promotes functional maturation of dendritic cells and displays adjuvant properties at the nasal mucosa level. Int Immunopharmacol 2009; 9:1366-73; PMID:19712757; http://dx.doi.org/10.1016/j.intimp.2009.08.010.
27. Shan F, Xia Y, Wang N, Meng J, Lu C, Meng Y, et al. Functional modulation of the pathway between dendritic cells (DCs) and CD4+T cells by the neuropeptide: methionine enkephalin (MENK). Peptides 2011; 32:929-37; PMID:21335041; http://dx.doi.org/10.1016/j.peptides.2011.01.033.
28. McLaughlin PJ, Sassani JW, Klocek MS, Zagon IS. Diabetic keratopathy and treatment by modulation of the opioid growth factor (OGF)-OGF receptor (OGFr) axis with naltrexone: a review. Brain Res Bull 2010; 81:236-47; PMID:19683562; http://dx.doi.org/10.1016/j.brainresbull.2009.08.008.
29. Hoyle CH. Evolution of neuronal signalling: transmitters and receptors. Auton Neurosci 2011; 165:28-53; PMID:20646967; http://dx.doi.org/10.1016/j.autneu.2010.05.007.
30. Zagon IS, Donahue RN, Bonneau RH, McLaughlin PJ. T lymphocyte proliferation is suppressed by the opioid growth factor ([Met(5)]-enkephalin)-opioid growth factor receptor axis: implication for the treatment of autoimmune diseases. Immunobiology 2011; 216:579-90; PMID:20965606; http://dx.doi.org/10.1016/j.imbio.2010.09.014.
31. Donahue RN, McLaughlin PJ, Zagon IS. Cell proliferation of human ovarian cancer is regulated by the opioid growth factor-opioid growth factor receptor axis. Am J Physiol Regul Integr Comp Physiol 2009; 296:R1716-25; PMID:19297547; http://dx.doi.org/10.1152/ajpregu.00075.2009.
32. Cheng F, Zagon IS, Verderame MF, McLaughlin PJ. The OGF-OGFr axis utilizes the p16 pathway to inhibit progression of human squamous cell carcinoma of the head and neck. Cancer Res 2007; 67:10511-8; PMID:17974995; http://dx.doi.org/10.1158/0008-5472.CAN-07-1922.
33. Cheng F, McLaughlin PJ, Verderame MF, Zagon IS. The OGF-OGFr axis utilizes the p21 pathway to restrict progression of human pancreatic cancer. Mol Cancer 2008; 7:5-17; PMID:18190706; http://dx.doi.org/10.1186/1476-4598-7-5.
34. Cheng F, McLaughlin PJ, Verderame MF, Zagon IS. The OGF-OGFr axis utilizes the p16INK4a and p21WAF1/CIP1 pathways to restrict normal cell proliferation. Mol Biol Cell 2009; 20:319-27; PMID:18923142; http://dx.doi.org/10.1091/mbc.E08-07-0681.
35. Zagon IS, Gibo DM, McLaughlin PJ. Zeta (zeta), a growth-related opioid receptor in developing rat cerebellum: identification and characterization. Brain Res 1991; 551:28-35; PMID:1655161; http://dx.doi.org/10.1016/0006-8993(91)90909-F.
36. Zagon IS, Verderame MF, McLaughlin PJ. The biology of the opioid growth factor receptor (OGFr). Brain Res Brain Res Rev 2002; 38:351-76; PMID:11890982; http://dx.doi.org/10.1016/S0165-0173(01)00160-6.
37. Klocek MS, Sassani JW, Donahue RN, McLaughlin PJ, Zagon IS. Regulation of Tenon's capsule fibroblast cell proliferation by the opioid growth factor and the opioid growth factor receptor axis. Invest Ophthalmol Vis Sci 2010; 51:5054-61; PMID:20463323; http://dx.doi.org/10.1167/iovs.09-4949.
38. McLaughlin PJ, Zagon IS, Park SS, Conway A, Donahue RN, Goldenberg D. Growth inhibition of thyroid follicular cell-derived cancers by the opioid growth factor (OGF) - opioid growth factor receptor (OGFr) axis. BMC Cancer 2009; 9:369; PMID:19835629; http://dx.doi.org/10.1186/1471-2407-9-369.
39. Jaglowski JR, Zagon IS, Stack BC Jr., Verderame MF, Leure-duPree AE, Manning JD, et al. Opioid growth factor enhances tumor growth inhibition and increases the survival of paclitaxel-treated mice with squamous cell carcinoma of the head and neck. Cancer Chemother Pharmacol 2005; 56:97-104; PMID:15791460; http://dx.doi.org/10.1007/s00280-004-0929-4.
40. Hua H, Lu C, Li W, Meng J, Wang D, Plotnikoff NP, et al.; HuiHua. Comparison of stimulating effect on subpopulations of lymphocytes in human peripheral blood by methionine enkephalin with IL-2 and IFN-γ. Hum Vaccin Immunother 2012; 8:1082-9; PMID:22854663.
41. Liu J, Chen W, Meng J, Lu C, Wang E, Shan F. Differentiation and Modulation of bone marrow progenitor of dendritic cell induced by methionine encephalin (MENK). Cancer Immunol Immmunother 2012
42. Chen W. Modulation of macrophage polarization promoting tumoricidal responses by neuropeptide: methionine encephalin (MENK). Cancer Immunol Immmunother 2012; http://dx.doi.org/10.1007/s00262-012-1240-6

43. Noh YW, Jang YS, Ahn KJ, Lim YT, Chung BH. Simultaneous in vivo tracking of dendritic cells and priming of an antigen-specific immune response. Biomaterials 2011; 32:6254-63; PMID:21620470.
44. Ronald N. Literature-related discovery: Potential treatments and preventatives for SARS. Technol Forecast Soc Change 2011; 78:1164-73; http://dx.doi.org/10.1016/j.techfore.2011.03.022.
45. Jara-Pérez JV, Berber A. Primary prevention of acute respiratory tract infections in children using a bacterial immunostimulant: a double-masked, placebo-controlled clinical trial. Clin Ther 2000; 22:748-59; PMID:10929921; http://dx.doi.org/10.1016/S0149-2918(00)90008-0.
46. Kammona O, Kiparissides C. Recent advances in nanocarrier-based mucosal delivery of biomolecules. J Control Release 2012; 161:781-94; PMID:22659331; http://dx.doi.org/10.1016/j.jconrel.2012.05.040.
47. Cherwonogrodzky JW. Research strategies for the treatment of biothreats. Curr Opin Pharmacol 2005; 5:465-72; PMID:16084772; http://dx.doi.org/10.1016/j.coph.2005.04.011.
48. Jeong YJ, Hong SW, Kim JH, Jin DH, Kang JS, Lee WJ, et al.; Young-JooJeong. Vitamin C-treated murine bone marrow-derived dendritic cells preferentially drive naïve T cells into Th1 cells by increased IL-12 secretions. Cell Immunol 2011; 266:192-9; PMID:21074755; http://dx.doi.org/10.1016/j.cellimm.2010.10.005.
49. Johansson C, Ingman M, Jo Wick M. Elevated neutrophil, macrophage and dendritic cell numbers characterize immune cell populations in mice chronically infected with Salmonella. Microb Pathog 2006; 41:49-58; PMID:16782300; http://dx.doi.org/10.1016/j.micpath.2006.03.004.
50. Hadeiba H, Lahl K, Edalati A, Oderup C, Habtezion A, Pachynski R, et al.; HuseinHadeiba. Plasmacytoid dendritic cells transport peripheral antigens to the thymus to promote central tolerance. Immunity 2012; 36:438-50; PMID:22444632; http://dx.doi.org/10.1016/j.immuni.2012.01.017.
51. Jung NC, Kim HJ, Kang MS, Lee JH, Song JY, Seo HG, et al. Photodynamic therapy-mediated DC immunotherapy is highly effective for the inhibition of established solid tumors. Cancer Lett 2012; 324:58-65; PMID:22554711; http://dx.doi.org/10.1016/j.canlet.2012.04.024.
52. Wu GF, Shindler KS, Allenspach EJ, Stephen TL, Thomas HL, Mikesell RJ, et al. Limited sufficiency of antigen presentation by dendritic cells in models of central nervous system autoimmunity. J Autoimmun 2011; 36:56-64; PMID:21095100; http://dx.doi.org/10.1016/j.jaut.2010.10.006.
53. Gottenberg JE, Chiocchia G. Dendritic cells and interferon-mediated autoimmunity. Biochimie 2007; 89:856-71; PMID:17562353; http://dx.doi.org/10.1016/j.biochi.2007.04.013.
54. Torres-Aguilar H, Blank M, Jara LJ, Shoenfeld Y. Tolerogenic dendritic cells in autoimmune diseases: crucial players in induction and prevention of autoimmunity. Autoimmun Rev 2010; 10:8-17; PMID:20678591; http://dx.doi.org/10.1016/j.autrev.2010.07.015.
55. Moyer JS, Maine G, Mulé JJ. Early vaccination with tumor-lysate-pulsed dendritic cells after allogeneic bone marrow transplantation has antitumor effects. Biol Blood Marrow Transplant 2006; 12:1010-9; PMID:17084367; http://dx.doi.org/10.1016/j.bbmt.2006.06.009.
56. Hashimoto D, Merad M. Harnessing dendritic cells to improve allogeneic hematopoietic cell transplantation outcome. Semin Immunol 2011; 23:50-7; PMID:21316261; http://dx.doi.org/10.1016/j.smim.2011.01.005.
57. Young JW, Merad M, Hart DN. Dendritic cells in transplantation and immune-based therapies. Biol Blood Marrow Transplant 2007; 13(Suppl 1):23-32; PMID:17222766; http://dx.doi.org/10.1016/j.bbmt.2006.10.023.
58. Ian S, Zagon MF, Verderame SS, Allen PJ. Cloning, sequencing, chromosomal wcation, and function of a cDNA encoding the opioid growth factor receptor (OGFR) in humans and a modulator of ogf activity in the growth of pancreatic and colorectal cancer. Gastroenterology 2000; 118:417; http://dx.doi.org/10.1016/S0016-5085(00)83780-4.
59. Avella DM, Kimchi ET, Donahue RN, Tagaram HR, McLaughlin PJ, Zagon IS, et al. The opioid growth factor-opioid growth factor receptor axis regulates cell proliferation of humanhepatocellular cancer. Am J Physiol Regul Integr Comp Physiol 2010; 298:459-66; http://dx.doi.org/10.1152/ajpregu.00646.2009.
60. McLaughlin PJ, Zagon IS, Park SS, Conway A, Donahue RN, Goldenberg D. Growth inhibition of thyroid follicular cell-derived cancers by the opioid growth factor (OGF) - opioid growth factor receptor (OGFr) axis. BMC Cancer 2009; 9:369; PMID:19835629; http://dx.doi.org/10.1186/1471-2407-9-369.
61. McLaughlin PJ, Levin RJ, Zagon IS. Opioid growth factor (OGF) inhibits the progression of human squamous cell carcinoma of the head and neck transplanted into nude mice. Cancer Lett 2003; 199:209-17; PMID:12969794; http://dx.doi.org/10.1016/S0304-3835(03)00341-0.
62. Di Renzo M, Pasqui AL, Bruni F, Saletti M, Bova G, Chiarion C, et al. The in vitro effect of pidotimod on some immune function in cancer patients. Immunopharm Immunot 1997; 19:37-51; http://dx.doi.org/10.3109/08923979709038532.
63. Castillo EA, Dea-Ayuela MA, Bolás-Fernández F, Rangel M, González-Rosende ME. The kinetoplastid chemotherapy revisited: current drugs, recent advances and future perspectives. Curr Med Chem 2010; 17:4027-51; PMID:20939823; http://dx.doi.org/10.2174/092986710793205345.
64. Ito A, Fujioka M, Tanaka K, Kobayashi T, Honda H. Screening of cytokines to enhance vaccine effects of heat shock protein 70-rich tumor cell lysate. J Biosci Bioeng 2005; 100:36-42; PMID:16233848; http://dx.doi.org/10.1263/jbb.100.36.
65. Kao JY, Zhang M, Chen CM, Pierzchala A, Chen JJ. Aberrant T helper cell response in tumor-bearing mice limits the efficacy of dendritic cell vaccine. Immunol Lett 2006; 105:16-25; PMID:16388858; http://dx.doi.org/10.1016/j.imlet.2005.11.026.
66. Frankenberger B, Schendel DJ. Third generation dendritic cell vaccines for tumor immunotherapy. Eur J Cell Biol 2012; 91:53-8; PMID:21439674; http://dx.doi.org/10.1016/j.ejcb.2011.01.012.
67. Cho D-Y, Yang W-K, Lee H-C, Hsu D-M, Lin H-L, Lin S-Z, et al. Adjuvant immunotherapy with whole-cell lysate dendritic cells vaccine for glioblastoma multiforme: a phase II clinical trial. World Neurosurg 2012; 77:736-44; PMID:22120301; http://dx.doi.org/10.1016/j.wneu.2011.08.020.
68. Hamdy S, Haddadi A, Hung RW, Lavasanifar A. Targeting dendritic cells with nano-particulate PLGA cancer vaccine formulations. Adv Drug Deliv Rev 2011; 63:943-55; PMID:21679733; http://dx.doi.org/10.1016/j.addr.2011.05.021.
69. Inaba K, Inaba M, Romani N, Aya H, Deguchi M, Ikehara S, et al. Generation of large numbers of dendritic cells from mouse bone marrow cultures supplemented with granulocyte/macrophage colony-stimulating factor. J Exp Med 1992; 176:1693-702; PMID:1460426; http://dx.doi.org/10.1084/jem.176.6.1693.